Optical spectroscopy and electronic band structure of ferromagnetic EuB_6

Jungho Kim and Young-June Kim
Department of Physics, University of Toronto, Toronto, Ontario, Canada M5S 1A7

J. Kuneš
Theoretical Physics III, Center for Electronic Correlations and Magnetism, Institute of Physics, University of Augsburg, D-86135 Augsburg, Germany

B. K. Cho
Department of Materials Science and Engineering and Center for Frontier Materials, K-JIST, Gwangju 500-712, Republic of Korea

E. J. Choi*
Department of Physics, University of Seoul, Seoul 130-743, Republic of Korea
(Received 4 September 2008; published 24 October 2008)

We present an optical conductivity of EuB_6 over a wide range (2 meV–5.5 eV) from reflectivity and ellipsometry measurements. Upon the ferromagnetic transition at $T_c=15.5$ K, interband transition $\sigma_1(\omega)$ decreases below $\omega=3.3$ eV and the lost spectral weight is transferred to the Drude $\sigma_1(\omega)$ at $\omega<0.33$ eV. Further a high-energy optical peak at around 4 eV exhibits a large splitting below T_c. We explain these high-energy $\sigma_1(\omega)$ changes, that is, spectral-weight recovery and peak splitting, using local-density approximation+U band-structure calculations. Our finding suggests strongly that: (1) EuB_6 is a semimetal and (2) the exchange-driven band splitting is the primary source of the drastic ω_p^2 change at $T<T_c$.

DOI: 10.1103/PhysRevB.78.165120 PACS number(s): 78.20.Ls, 71.20.Eh, 71.70.Gm, 78.40.Kc

I. INTRODUCTION

The interaction of itinerant carriers with localized magnetic moments can give rise to an order-of-magnitude change in resistivity following magnetic ordering, the so-called colossal magnetoresistance, as seen, for example, in EuO, (Ga,Mn)As, or $La_{0.7}Ca_{0.3}MnO_3$. Europium hexaboride (EuB_6) is another material exhibiting this technologically important behavior. In EuB_6 low-concentration charge carriers ($n\sim10^{19}$ cm^{-3}) coexists with local Eu $4f$ moments of purely spin origin ($S=7/2$). Ferromagnetic (FM) transition at $T_c=15.5$ K is accompanied by an order-of-magnitude drop in resistivity[1] and a factor-of-2 increase in the plasma frequency ω_p.[2] Simple crystal structure and frozen $4f$ orbital degrees of freedom make EuB_6 free from complications such as Jahn-Teller effect or orbital ordering typical of manganites. However, despite considerable experimental and theoretical effort, the understanding of the EuB_6 physics is far from settled.

The complications and controversy stem from a seemingly simple band structure characterized by a "gap" of about 2 eV inside which a single valence band (VB) and a conduction band (CB) approach each other. The key to understanding of EuB_6, whether they actually cross, is still not satisfactorily answered. Angle-resolved photoemission spectroscopy (ARPES) (Ref. 3) made a strong case for the semiconductor picture reporting a sizable gap of 1 eV, implying that the metallic reflectivity,[2] de Haas–van Alphen, and Shubnikov–de Haas signals[4,5] reported earlier are due to extrinsic carriers. However, more recent ARPES (Ref. 6) experiments reveal VB crossing the Fermi level, explaining the previous observation by surface effects. The band-structure theory does not provide an unambiguous answer either. The local-density approximation (LDA) predicts EuB_6 to be a semimetal with VB and CB overlapping in the vicinity of X point of the Brillouin zone.[7,8] A well-known failure of LDA for another divalent hexaboride, CaB_6, which is predicted to be a semimetal, while other techniques such as GW (Ref. 9) or weighted density approximation (Ref. 10) find an ~1 eV gap in agreement with experiment, teaches us to accept this result with caution.

In this work, we use reflectivity and ellipsometry measurements to study the temperature dependence of the optical spectrum of EuB_6 over a wide frequency range of 2 meV–5.5 eV. Following on the work of Degiorgi *et al.*,[2] who reported more than doubling of the plasma frequency ω_p upon FM ordering, we address the question of where the enhancement of the Drude weight comes from. Our main experimental result is that this additional spectral weight is transferred mostly from the high-frequency region of 1–3 eV. We discuss the existing theoretical proposals in the context of this observation and present numerical simulation of the spectral-weight transfer as described by static mean-field LDA+U approach.

II. EXPERIMENT

Single-crystal EuB_6 samples were synthesized by the borothermal flux method and characterized by x-ray-diffraction, dc-resistivity, and magnetization measurements.[11,12] The normal-incidence reflectivity $R(\omega)$ on the polished surface of the crystal, which was mounted on optically black cones in a cold-finger flow cryostat, was measured at 5 K$\leq T\leq$100 K in the 2 meV–1 eV range using a Fourier-transform spectrometer with the *in situ* overcoating technique.[13] The pressure was kept on the order of 10^8 torr. For the 0.7–5.5 eV range, the optical dielectric constant

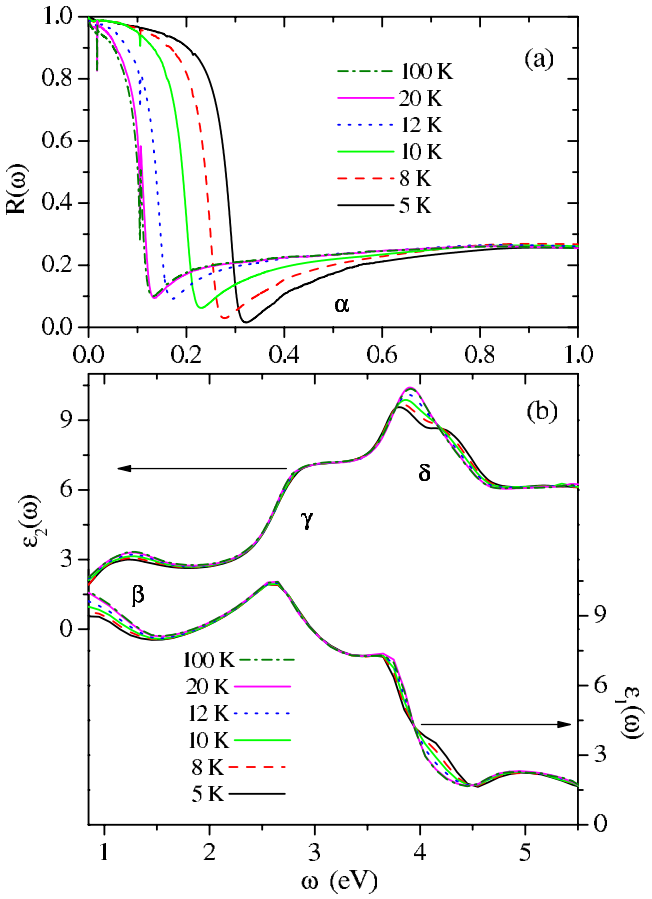

FIG. 1. (Color online) Optical spectra of EuB_6 for T=5, 8, 10, 12, 20, and 100 K. (a) Reflectivity for $\omega < 1$ eV. (b) Real $\varepsilon_1(\omega)$ and imaginary $\varepsilon_2(\omega)$ parts of the dielectric constant for 0.7 eV$< \omega <$5.5 eV from the ellipsometry measurement.

$\varepsilon(\omega)=\varepsilon_1(\omega)+i\varepsilon_2(\omega)$ was obtained using spectroscopic ellipsometer (Woollam VASE) at an angle of incidence of 70°. The window strain effect has been corrected using a standard Si wafer. The polished sample was mounted at the helium-flow cryostat's cold finger with the radiation shield. The pressure was kept on the order of 10^9 torr to avoid fictitious effects due to adsorbed gases on the sample surface. Much care was taken in reducing absorbed gases on the sample surface. While the radiation shield and the whole cold-finger assembly were still cold, the sample temperature was ramped above room temperature to clean the sample surface and transfer the absorbed gases on the sample surface to the still-cold cryostat parts. This procedure was repeated several times. Throughout the optical measurements, sample temperature was controlled within 0.1 K of stability.

III. RESULTS AND DISCUSSION

A. Experimental

Figure 1(a) shows $R(\omega)$ of EuB_6 in the 5 K$\leq T \leq$100 K range. High reflectivity in the low-frequency region is due to the metallic Drude response. The plasma edge shifts to higher energy as T decreases below 20 K, which is consistent with the earlier report by Degiorgi *et al.*[2] The

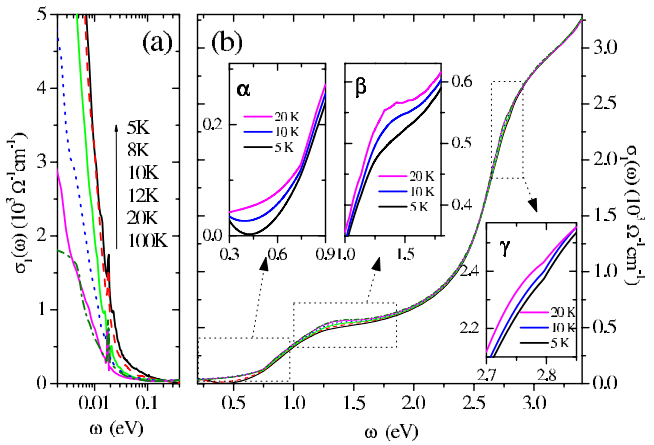

FIG. 2. (Color online) Optical conductivities $\sigma_1(\omega)$ of EuB_6 for (a) Drude part at $\omega < 0.33$ eV and (b) IB part at 0.33 eV$< \omega <$3.3 eV. The insets in (b) are close-up views of the three features α, β, and γ.

complex dielectric constant $\varepsilon_{1,2}(\omega)$ from the high-frequency ellipsometry is shown in Fig. 1(b). It shows three absorption peaks at 1.4, 3, and 4 eV (labeled as β, γ, and δ, respectively) which represent the interband (IB) electronic transitions. The peaks exhibit weak but systematic changes with temperature. Remarkably larger change is observed at $\omega > 4$ eV (δ feature) which is greater than 10^3 of the temperature scale.

To investigate the T-dependent spectral-weight transfer, we extract the optical conductivity $\sigma_1(\omega)$ from $R(\omega)$ and $\varepsilon_{1,2}(\omega)$ using the Kramers-Kronig (KK) constrained variational fitting method.[14] Figure 2 shows the low-frequency Drude part of $\sigma_1(\omega)$ (a) well separated from the high-frequency spectrum (b). For quantitative analysis we define the Drude weight $S_{\text{Drude}}=8\int_0^{\omega_c} d\omega\sigma_1(\omega)$ and the high-frequency spectral weight $S(\Omega)=8\int_{\omega_c}^{\Omega} d\omega\sigma_1(\omega)$, where ω_c is set to 0.33 eV and the prefactor is chosen so that $S_{\text{Drude}}=\omega_p^2$. The Drude weight above the FM transition temperature T_c is hardly T dependent, giving $\omega_{p,\text{PM}}\sim 3300$ cm^{-1}, while for $T<T_c$ it increases to obtain $\omega_{p,\text{FM}}^2/\omega_{p,\text{PM}}^2\sim 4.4$ at 5 K. On the other hand, as mentioned above, the high-frequency $\sigma_1(\omega)$ (β and γ) exhibits an opposite behavior, that is, a decrease in $\sigma_1(\omega)$ all the way up to 3.3 eV.

In order to analyze the redistribution of the spectral weight, we plot the difference $\Delta\sigma_1(\omega,T)=\sigma_1(\omega,T)-\sigma_1(\omega,100\text{ K})$ in Fig. 3(a). The high-frequency part of $\Delta\sigma_1(\omega,T)$ is negative all the way up to ~3.3 eV. The increase in ΔS_{Drude} with decreasing temperature is within the experimental accuracy compensated by the decrease in $\Delta S(\Omega=3.3\text{ eV})$ as shown in Fig. 3(b). The uniform sign of $\Delta\sigma_1(\omega,T)$ throughout the 0.33 eV$<\omega<$3.3 eV range and recovery of the spectral weight only upon integration up to 3.3 eV is the main experimental result of this work.

In Fig. 4(a), we show the detailed temperature dependence of the high-energy peak δ at around 4 eV. The data were taken with a 1 K step between 4.2 and 20 K. δ consists of a single peak at 3.9 eV in the paramagnetic (PM) state ($T>T_c$) and splits to two peaks in the FM state ($T<T_c$). Figure 4(b) shows that the splitting which amounts to 0.48

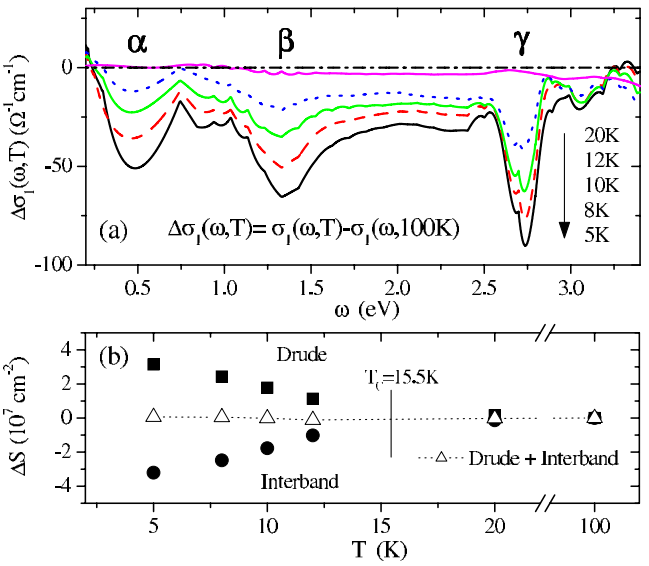

FIG. 3. (Color online) (a) The change in conductivity with temperature, $\Delta\sigma_1(\omega,T)=\sigma_1(\omega,T)-\sigma_1(\omega,100\ \mathrm{K})$. (b) The spectral-weight change $\Delta S=8\int\Delta\sigma_1(\omega)d\omega$ of the Drude part ($0<\omega<0.33$ eV) and the interband part (0.33 eV$<\omega<$3.3 eV) as a function of temperature.

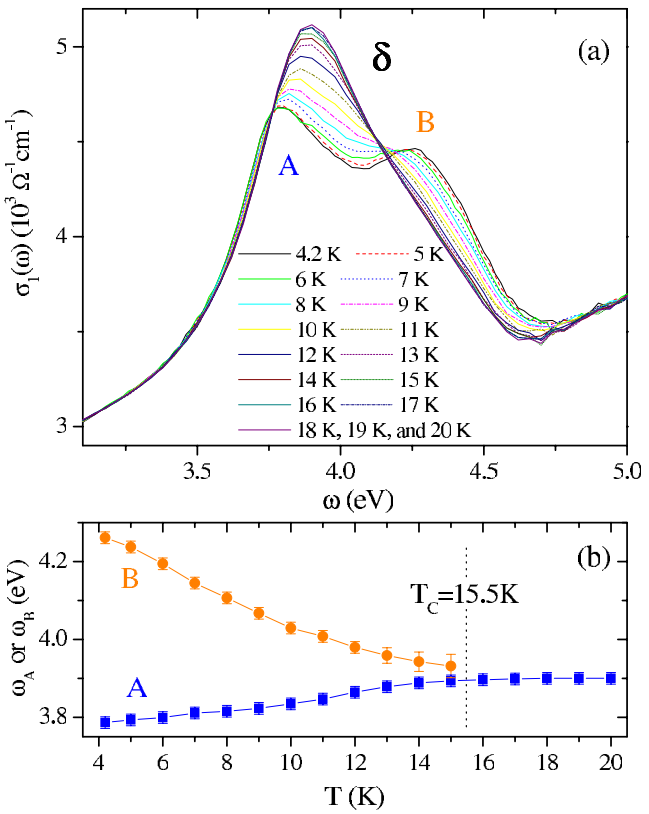

FIG. 4. (Color online) (a) Interband transition δ and its T-dependent changes for $T<20$ K. The data were taken with a 1 K step. (b) Peak position plot as a function of T. This plot clearly shows that the splitting is correlated with the FM transition at $T_c=15.5$ K.

eV at $T=4.2$ K is correlated with the FM transition. This large T-dependent change in the δ peak is localized within this feature and does not involve spectral-weight transfer from the Drude part.

The theoretical models proposed to describe EuB_6 can be divided into: (i) one-band models involving dynamic many-body effects and (ii) static multiband models. In theories (i) band occupation does not change between the FM and PM phases and the variation in ω_p and the transport properties are ascribed to the changed character of the electronic states. These theories do not distinguish between intrinsic and extrinsic (impurity) origins of the carriers. In theories (ii) multiple bands are crucial since the band occupation changes between the FM and PM phases. It should be pointed out that the discussed models are not necessarily mutually exclusive.

First, we discuss the one-band theories starting with the model of Pereira *et al.*[15] Increasing temperature leads to increasing fluctuations of the local moments, which are modeled by a quenched disorder and the increase in resistivity in PM phase is attributed to the localization phenomena. While this model may be relevant for the transport properties, it does not explain the observed behavior of low-frequency optical conductivity. Allen *et al.*[16] studied the effect of increasing disorder strength on the optical conductivity, finding a continuous deformation of the Drude peak consisting of a shift of its maximum to a finite frequency while preserving the total spectral weight. In EuB_6 a qualitatively different behavior is observed: at all temperatures the Drude peak is well defined and separated from the rest of the spectrum, while its total weight is reduced. Another argument against the disorder model is the frequency scale of the spectral-weight recovery (~3 eV). Since the disorder does not change the band occupation, the total weight of intraband contribution is expected to be unchanged and contained within the frequency range of Drude peak plus the disorder strength ($\leq JS\sim 0.5$ eV). The high-frequency interband contribution to $\Delta\sigma_1(\omega)$ is then expected to oscillate with zero total spectral weight.

Another one-band proposal involves the quasi-particle (QP) renormalization and spectral-weight transfer due to formation of magnetic polarons. The optical spectral-weight transfer due to dynamic renormalization effects is widely seen in strongly correlated electron materials, which reflects the redistribution of spectral weight between coherent QPs and incoherent local excitations, magnetic polarons in the case of EuB_6. In this scenario the optical spectral weight is recovered on the energy scale of magnetic polaron formation, $JS\sim 0.5$ eV. The argument of high-frequency scale of the spectral-weight recovery observed in experiment applies as in the disorder model. Kreissl and Nolting[17] studied a two-band Kondo lattice model with realistic parameters, which includes both the dynamic renormalization and the static multiband effect. They found only moderate QP renormalization and concluded that the static mean-field part of their theory plays the dominant role.

B. Computational

In the following we discuss in detail the multiband scenario. Using LDA+U band-structure calculation, the authors

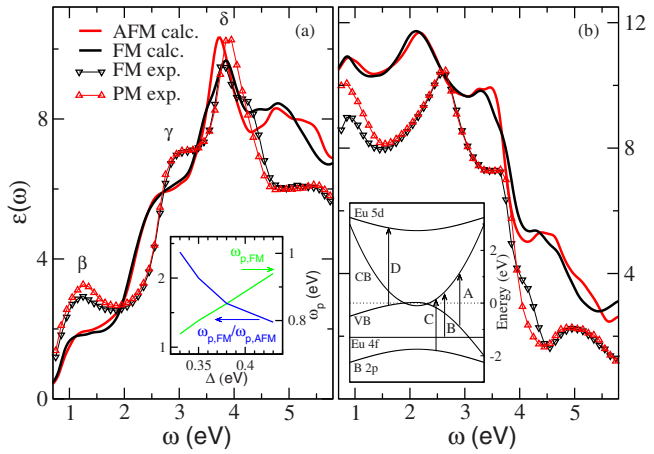

FIG. 5. (Color online) The real and imaginary parts of the dielectric constant are obtained from the ellipsometry measurements (line+symbols) and LDA+U calculation (line). The inset in left panel shows the dependence of the plasma frequency in FM state, ω_p^{FM}, and of the ratio $\omega_p^{\mathrm{FM}}/\omega_p^{\mathrm{AFM}}$ vs the VB/CB overlap measured for majority spin in FM state. The inset in right panel shows the schematic plot of the EuB_6 band structure.

of Ref. 8 observed that the VB/CB overlap, if it exists, is polarization dependent, which may lead to increase in ω_p in FM state. In order to discuss this polarization-shift scenario in detail, we have extended the LDA+U calculations in Ref. 8 to obtain the optical spectra.[18] The PM state is modeled by antiferromagnetic (AFM) arrangement of $4f$ local moments, which removes the net polarization but leaves the band topology around X point intact. The interband FM and AFM spectra are compared to the experimental ones in Fig. 5. The observed features can be understood with help of the band-structure scheme in the inset of Fig. 5. The first prominent feature β between 1 and 2 eV is due to transitions (marked as B) from the flat $4f$ band into CB. The shoulder γ arises mostly from transitions (C) between lower-lying occupied bands and VB with some contribution from transitions (A) between VB and CB. Finally, the δ peak originates from transitions (D) between VB and a flat Eu $5d$ band. Vanishing hybridization between VB and CB in the vicinity of X point[8,19] leads to a negligible amplitude for dipole transitions below 1 eV.

Next, we address the difference between FM and AFM spectra. The band theory captures well the redistribution of the spectral weight within the δ peak, which arises from spin polarization of the Eu $5d$ band. However, we do not find any appreciable variation in the plasma frequency as $\omega_p^{\mathrm{AFM}} \sim \omega_p^{\mathrm{FM}}=1.6$ eV, which is moreover a factor of 2 larger than the experimental FM value. A plausible explanation is overestimation of the band overlap. Quite generally, ω_p may depend appreciably on the spin polarization only if the band overlap is comparable to the polarization splitting, in which case the band occupancies vary nonlinearly with the spin polarization. We found that a 0.43 eV rigid shift of CB yields $\omega_p^{\mathrm{FM}}/\omega_p^{\mathrm{AFM}}=2$ and $\omega_p^{\mathrm{FM}}=0.80$ eV, in fair agreement with experimental values. As shown in Fig. 5 the two quantities are rather sensitive to the band overlap and thus fitting both simultaneously is a nontrivial result.

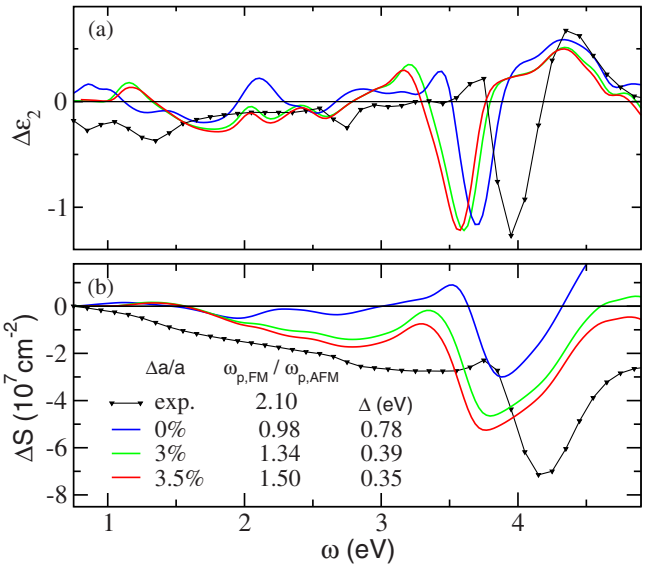

FIG. 6. (Color online) (a) The difference in the absorptive part of dielectric constant between the FM and AFM solutions for various lattice expansions compared to the difference between experimental values obtained at 5 K (FM) and 100 K (PM). Panel (b) shows the corresponding integrated conductivity difference ΔS. Δ denotes the band overlap defined as in Fig. 4.

To investigate the connection between the Drude weight and interband spectrum, a rigid band shift is not useful since it violates the optical sum rule. On the other hand, a moderate lattice expansion can reduce the band overlap while keeping the band topology unchanged. Importantly, the optical sum rule is fulfilled. In Fig. 6(a) we show the difference between the FM and AFM absorption spectra, $\Delta\epsilon_2(\omega)$, for various lattice expansions. The 0% $\Delta\epsilon_2(\omega)$ oscillates about zero and the corresponding optical conductivity integrates to zero over the $\beta-\gamma$ features. Upon increasing the $\omega_p^{\mathrm{FM}}/\omega_p^{\mathrm{AFM}}$ ratio (by lattice expansion), $\Delta\epsilon_2$ becomes negative over the entire $\beta-\gamma$ region and the magnitude of the spectral-weight transfer $\Delta S(\Omega)$ [Fig. 6(b)] increases.

In principle a nonzero difference spectrum may arise from weight redistribution within the IB transitions, as for the 0%-expansion, but for the expanded lattice with a reduced gap this is not the case. Although the lattice expansion was introduced as a poor man's correction to the overestimated LDA band overlap, the ability to manipulate the band overlap without violating optical sum rule allows us to demonstrate correlation between the change in plasma frequency and the change in the spectral weight in the $\beta-\gamma$ region. This shows that the spectral-weight transfer from the $\beta-\gamma$ region arises from the reduction of the phase space available for the corresponding optical transitions resulting from variation in the VB and CB occupancies upon spin polarization. Note that the effect takes place only for a small AFM band overlap to start with. For large overlap, as in the case of 0% expansion, the spin polarization does not affect the total VB and CB populations and thus no sizable changes in the plasma frequency or integrated $\beta-\gamma$ spectral weight take place.

We have not mentioned the α feature so far. The α peak is completely missing in the calculated spectra due to a very small amplitude of the interband transitions below 1 eV.

Given the width and position of the α peak, a plausible explanation may be an intraband contribution from magnetic polaron formation. An unambiguous understanding of this feature is, however, beyond the capability of the presented theory.

So far, we have established that the observed changes in the optical spectrum arise primarily from changes in the VB or CB occupancies. Our numerical simulations show that polarization-dependent band overlap of VB and CB provides explanation of these changes. Alternatively, one can imagine a scenario in which the majority-spin CB crosses upon spin polarization a narrow impurity band, similar to the famous metal-insulator transition in Eu-rich EuO.[20] In such a case, one expects a rather abrupt change in the optical spectrum at the point where the chemical potential crosses the impurity band. This is quite different from a continuous evolution of the spectrum that we observe (see Fig. 3).

IV. CONCLUSION

In conclusion, using reflectivity and ellipsometry measurements we have studied the transfer of optical spectral weight in EuB_6 upon magnetic ordering. We have shown that the increase of Drude weight in FM phase is compensated over an energy region reaching up to 3 eV. In addition, a high energy optical peak at around 4 eV splits to two peaks in FM state. We have critically discussed various theoretical scenarios and shown that the semimetallic band structure with a band overlap, reduced compared to the LDA+U, value can consistently describe the substantial high-frequency part of the spectral-weight transfer, while the dynamical many-body effects are limited to the region below 1 eV. Our techniques do not address the transport properties and therefore our conclusions do not exclude the relevance of the discussed theories for description of the dc conductivity or Hall effect.

ACKNOWLEDGMENTS

The authors thank C. C. Homes for helping in reflectivity measurement. J.K. would like to thank D. Vollhardt, L. Baldassare, and K. Byczuk for illuminating discussions. This work was supported by KRF Grant No. 070-C00032 and the KOSEF through CSCMR. The work at Toronto was supported by NSERC Discovery Grant and Research Tools and Instrumentation Grant. J.K. acknowledges the support of SFB 484 of the Deutsche Forschungsgemeinschaft. The works of GIST was supported by the Korean Foundation Grant funded by the Korean Government (MOEHRD, Basic Research Promotion Fund) (KRF-2007-313-C00254).

*Corresponding author. echoi@uos.ac.kr

[1] C. N. Guy, S. von Molnar, J. Etourneau, and Z. Fisk, Solid State Commun. **33**, 1055 (1980).
[2] L. Degiorgi, E. Felder, H. R. Ott, J. L. Sarrao, and Z. Fisk, Phys. Rev. Lett. **79**, 5134 (1997).
[3] J. D. Denlinger, J. A. Clack, J. W. Allen, G.-H. Gweon, D. M. Poirier, C. G. Olson, J. L. Sarrao, A. D. Bianchi, and Z. Fisk, Phys. Rev. Lett. **89**, 157601 (2002).
[4] R. G. Goodrich, N. Harrison, J. J. Vuillemin, A. Teklu, D. W. Hall, Z. Fisk, D. Young, and J. Sarrao, Phys. Rev. B **58**, 14896 (1998).
[5] M. C. Aronson, J. L. Sarrao, Z. Fisk, M. Whitton, and B. L. Brandt, Phys. Rev. B **59**, 4720 (1999).
[6] J. D. Denlinger, F. Wang, J. W. Allen, Han-Oh Lee, Z. Fisk, B. Delley, and R. Monnier, APS Meeting Bulletin, 2007 (unpublished), Paper No. A7.00003.
[7] S. Massidda, A. Continenza, T. M. Pascale, and R. Monnier, Z. Phys. B: Condens. Matter **102**, 83 (1996).
[8] J. Kuneš and W. E. Pickett, Phys. Rev. B **69**, 165111 (2004).
[9] W. Ku and A. G. Eguiluz, Phys. Rev. Lett. **89**, 126401 (2002).
[10] Z. Wu, D. J. Singh, and R. E. Cohen, Phys. Rev. B **69**, 193105 (2004).
[11] J.-S. Rhyee, B. K. Cho, and H.-C. Ri, Phys. Rev. B **67**, 125102 (2003).
[12] J.-S. Rhyee, B. H. Oh, B. K. Cho, H. C. Kim, and M. H. Jung, Phys. Rev. B **67**, 212407 (2003).
[13] C. C. Homes, M. Reedyk, D. A. Crandles, and T. Timusk, Appl. Opt. **32**, 2976 (1993).
[14] A. B. Kuzmenko, Rev. Sci. Instrum. **76**, 083108 (2005).
[15] V. M. Pereira, J. M. B. Lopes dos Santos, E. V. Castro, and A. H. Castro-Neto, Phys. Rev. Lett. **93**, 147202 (2004).
[16] S. J. Allen, D. C. Tsui, and F. DeRosa, Phys. Rev. Lett. **35**, 1359 (1975).
[17] M. Kreissl and W. Nolting, Phys. Rev. B **72**, 245117 (2005).
[18] P. Blaha, K. Schwarz, G. K. H. Madsen, D. Kvasnicka, and J. Luitz, *WIEN2K, An Augmented Plane Wave Plus Local Program for Calculating Crystal Properties* (Technical University Wien, Austria, 2001).
[19] C. O. Rodriguez, R. Weht, and W. E. Pickett, Phys. Rev. Lett. **86**, 1142 (2001).
[20] J. B. Torrance, M. W. Shafer, and T. R. McGuire, Phys. Rev. Lett. **29**, 1168 (1972).